Chemical Science

ROYAL SOCIETY OF CHEMISTRY

EDGE ARTICLE

View Article Online
View Journal

Cite this: DOI: 10.1039/d5sc09759b

All publication charges for this article have been paid for by the Royal Society of Chemistry

Near-infrared-to-deep-blue photon upconversion engineered from PbS quantum dots and perylene derivatives

Hongyu Li,†[a] Qingxin Luan,†[a] Shuai Zhang,[a] Lin Xi,[a] Yanan Feng[a] and Lili Hou *[ab]

Received 12th December 2025
Accepted 16th February 2026

DOI: 10.1039/d5sc09759b

rsc.li/chemical-science

Near-infrared (NIR)-to-visible light triplet–triplet annihilation photon upconversion (TTA-UC) holds great promise for solar energy harvesting, photochemistry, and bioimaging. However, achieving a large apparent anti-Stokes shift from the NIR to the blue region remains highly challenging. Here, we present the first TTA-UC system that can upconvert NIR excitation beyond 800 nm with emission approaching the deep-blue spectral region. This performance is realized by precisely engineering the triplet energy levels within only 0.06 eV among PbS quantum dots (QDs) as sensitizers, perylene-3-carboxylic acid (3-PYCA) as a novel mediator and perylene as an annihilator. The system exhibits an exceptional anti-Stokes shift of up to 1.3 eV, representing both a record performance to date and the maximum for QD-based TTA-UC systems. Meanwhile, a high TTA-UC quantum yield of 2.1% (out of a 50% maximum) is achieved, which is an order of magnitude higher than that of previously reported QD-based systems exhibiting anti-Stokes shifts above 0.8 eV. Moreover, the upconverted deep-blue light enables efficiently activated *cis*-to-*trans* photoisomerization of azobenzene (Azo), demonstrating the high potential in NIR light triggered photochemical transformation.

Introduction

Upconversion (UC) of low-energy photons to high-energy photons has been widely applied in solar energy harvesting,[1–4] biological imaging,[5,6] optoelectronic devices[7] and additive manufacturing.[8,9] Recent progress in the design of lanthanide-based upconversion nanoparticles (UCNPs) and nonlinear optical strategies offers the possibility of achieving large anti-Stokes shifts, enabling the conversion of near-infrared (NIR) photons into ultraviolet (UV) emission.[10–12] However, these approaches require the use of high-intensity coherent light sources, and the upconversion efficiencies remain very low (generally less than 1%). Triplet–triplet annihilation photon upconversion (TTA-UC), which employs energy-matched pairs of a photosensitizer and an annihilator, is considered as one of the most attractive approaches due to its high UC quantum yields (UCQYs) and ability to convert low-intensity and incoherent light, such as solar radiation.[13] Quantum dot (QD)-based TTA-UC has attracted increasing research attention and achieved rapid progress in recent years.[14] Compared to organic sensitization, QDs offer many advantages, including size-tunable energy levels, broad absorption spectra, high molar extinction coefficients, and strong spin–orbit coupling, which are keys to efficiently sensitize molecular triplets.[15–19] QD-based TTA-UC typically consists of three components: QDs, mediators and annihilators. The QDs absorb incident low-energy photons, then transfer the energy to mediators anchored on their surface *via* the first triplet energy transfer (TET_1) process. The yielded long-lived triplet excited state of the mediators (on the timescale of microseconds to milliseconds) allows the second triplet energy transfer (TET_2) step to the annihilators. Triplet–triplet annihilation occurs when two annihilators in their excited triplets encounter each other, wherein one annihilator transfers to its singlet excited state from where a high-energy photon emits, and the other relaxes to the ground state.

The apparent anti-Stokes shift in TTA-UC represents a key parameter that demonstrates the energy difference between upconverted and the excitation photons. It theoretically limits to twice the sensitizer's triplet energy minus the annihilator singlet energy. In principle, it allows to upconvert near-infrared light (NIR, >780 nm, <1.59 eV) into the deep-blue region (430–460 nm, 2.69–2.88 eV) with an anti-Stokes shift up to 1.3 eV, thereby enabling access to many high-energy photoactivated processes, such as photoisomerization, photocatalysis, and bioimaging with deep penetration. Considerable research has been devoted to designing TTA-UC from the NIR region with large anti-Stokes shift in the last two decades.[13,20] For example, Castellano *et al.* reported a conjugated supramolecular metal complex (Pyr_1RuPZn_2) that upconverted 780 nm light to green

[a]*School of Precision Instruments and Optoelectronics Engineering, Key Laboratory of Optoelectronics Information Technology, Tianjin University, Tianjin 300072, China. E-mail: lilihou@tju.edu.cn*

[b]*Department of Chemistry and Chemical Engineering, Chalmers University of Technology, Gothenburg 412 96, Sweden*

† H. L. and Q. L. contributed equally to this work.

emission with an anti-Stokes shift of 0.86 eV and UCQYs approaching 0.4% (out of a maximum of 50%).[21] Kimizuka *et al.* designed an Os complex (D1) as a photosensitizer and rubrene as an annihilator,[22] which enables UC of 935 nm to yellow emission with an anti-Stokes shift up to 0.86 eV and UCQYs of ~0.22%. Chen *et al.* reported that non-organometallic cyanine sensitizers with high molar extinction coefficients ($\varepsilon > 10^5$ M^{-1}) at 808 nm, when paired with red annihilators, achieved UCQYs of up to 1.73%.[23] Despite these advancements, it remains challenging for molecular sensitizers to absorb NIR photons beyond 800 nm and subsequently drive efficient TTA-UC with anti-Stokes shifts over 1.0 eV and UCQYs above 1%. This is mainly due to energy-matching constraints, energy loss during the intersystem crossing (ISC) process, and increased non-radiative decay of molecules in the NIR regime. QD-based TTA-UC can theoretically achieve larger anti-Stokes shift because of the small singlet-triplet splitting of the QDs and the facile access of their absorption and triplet levels into the NIR region.[14] Recently, Pang *et al.* reported PbS QDs capped with thiophene-substituted diketopyrrolopyrrole (Th-DPP) derivatives as mediators, enabling the UC of 1064 nm excitation to yellow emission of rubrene with an anti-Stokes shift of 1.07 eV and a UCQY of ~0.18%.[24] Deng *et al.* utilized lanthanide-doped nanocrystals with porphyrin derivatives as mediators, achieving a maximum anti-Stokes shift of 1.1 eV, but with a very low UCQY (<0.001%).[25] The challenges in QD-based TTA-UC lie not only in developing non-toxic based QDs for sustainability and improving QD quality by suppressing surface traps and non-radiative pathways, but also in engineering the surface ligand chemistry to enable stable and efficient Dexter energy transfer. Specifically, when aiming for upconversion of NIR light into the deep-blue region with an anti-Stokes shift approaching 1.3 eV and enhanced UCQY, it demands precise energetic engineering of the QD sensitizer–mediator ligand–annihilator assembly to efficiently harvest NIR photons, minimize energy losses and maximize triplet exciton generation.

Here, we report the first example of a NIR-to-deep-blue TTA-UC system composed of PbS QDs and commercially available perylene derivatives, achieving an anti-Stokes shift of up to 1.3 eV (Fig. 1), which, to the best of our knowledge, represents the highest value reported to date for TTA-UC systems.[20] This performance is realized by precisely engineering the triplet energy alignment between the QDs, mediator, and annihilator within a 0.06 eV bandgap. Perylene-3-carboxylic acid (3-PYCA) was first introduced as a surface-bound mediator on PbS QDs, relaying triplet energy from the QDs to perylene, which acts as the annihilator. The triplet state of 3-PYCA lies slightly below that of PbS QDs, while enabling a highly efficient TET_1 (>90%) process. The resulting triplet-excited 3-PYCA then undergoes endergonic TET_2 to the perylene triplet state, followed by triplet–triplet annihilation that generates deep-blue emission from the singlet excited state of perylene (S_1 = 2.83 eV) under 808 nm (1.53 eV) excitation of PbS QDs. The NIR-to-deep-blue UCQY was determined to be 2.1%, surpassing those of all previously reported QD-based TTA-UC systems exhibiting anti-Stokes shifts above 0.8 eV (Table S1). Furthermore, our system enables efficient NIR activated photochemistry, as demonstrated by the successful *cis*-to-*trans* photoisomerization of azobenzene (Azo) under 808 nm irradiation without the need for direct blue or violet excitation.

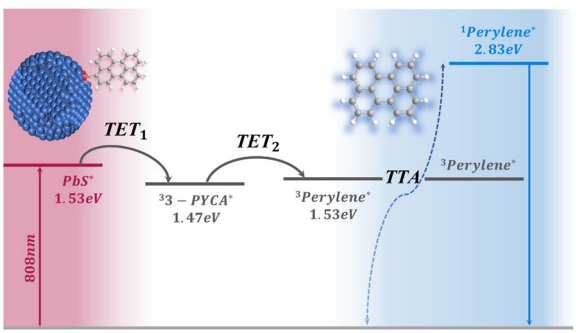

Fig. 1 Schematic of the NIR-to-deep-blue TTA-UC system containing PbS QDs, 3-PYCA as the mediator and perylene as the annihilator. 1.53 eV corresponds to the photon energy of 808 nm excitation in PbS QDs. The lowest excited singlet state of perylene is calculated from experiments, and the lowest excited triplet states of 3-PYCA and perylene are estimated from density functional theory calculations (see the SI for calculation details and estimation of energy levels).

Results and discussion

Absorption and emission properties

The chemical structures and spectra of commercially available perylene and 3-PYCA are shown in Fig. 2a. Perylene is a typical annihilator that is commonly paired with sensitizers that absorb in the visible region. Individual vibration energy levels of the ground and singlet excited states of perylene cause well-resolved vibronic structure observed in photoluminescence (PL) spectra, with the main emission bands located in the deep-blue region.[26,27] The photoluminescence quantum yields (PLQYs) of perylene is reported to be unity in a dilute solution.[28] However, as an annihilator, the typically used concentrations are above 1 mM, therefore the concentration-dependent absorption, PL spectra and PLQY of perylene were also determined and are shown in Fig. S1 and Table S2. When the concentration of perylene is over 1 mM, the light below 450 nm is strongly absorbed and the first emission band at 450 nm was attenuated due to the inner-filter effect. No additional emission band appeared at longer wavelength indicating the absence of excimer formation even at a concentration of 20 mM.[29] The decrease in PLQY to 75% at 10 mM and 45% at 20 mM is mainly attributed to aggregation-induced PL quenching. The PL lifetime of dilute perylene was determined to be 4.05 ns in toluene as reported (Fig. S2).[30] Introduction of a carboxyl functional group into perylene reduces its characteristic features in both absorption and photoluminescence spectra, and induces spectral red shift due to reduced vibrational activity and lower energy levels.[31] The S_1 energies of perylene and 3-PYCA are 2.83 eV and 2.67 eV, respectively, determined from the crossing point of their normalized absorption and emission spectra in Fig. 2a. The density functional theory (DFT) calculations yield corresponding S_1 values of 2.73 eV for perylene and 2.55 eV for 3-PYCA, with an estimated uncertainty of approximately 0.1 eV.

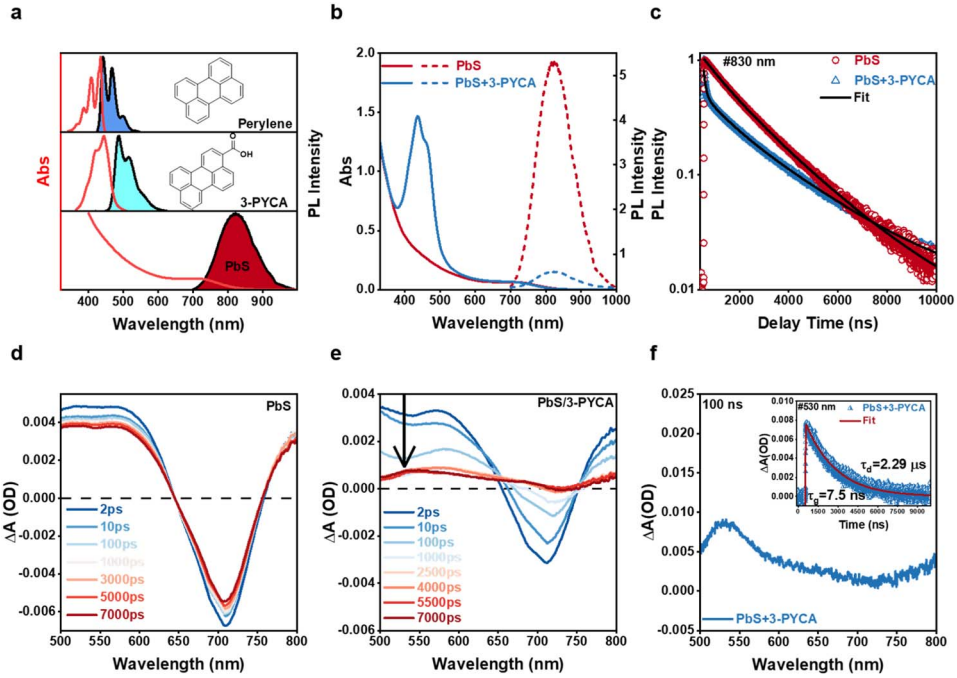

Fig. 2 (a) Absorption and PL (red and black lines, respectively) spectra of perylene, 3-PYCA, and PbS QDs. (b) Absorption, PL spectra, and (c) time-resolved PL decay at 830 nm of PbS QDs with and without the 3-PYCA ligand. The femtosecond TA spectra of (d) PbS QDs and (e) PbS QDs with 3-PYCA between 2 ps and 7000 ps. (f) The nanosecond TA spectra of PbS QDs with 3-PYCA at a time delay of 100 ns. The inset shows the time-resolved triplet signal decay of PbS QDs with 3-PYCA at 530 nm.

The calculated T_1 energies are 1.53 eV for perylene (consistent with the reported value)[32] and 1.47 eV for 3-PYCA (Table S3). Although the absolute T_1 energy level may slightly deviate due to the inherent uncertainty of DFT calculation, the relative energy difference between perylene and 3-PYCA of 0.06 eV is considered reliable. The PLQY of 3-PYCA was determined to be 20% with a PL lifetime of 4.56 ns in toluene (Fig. S2). In order to match the triplet energy of 3-PYCA and access NIR excitation over 800 nm, PbS QDs were synthesized to obtain the desired absorption band (Section 1.2 in the SI).[33] The size of synthesized PbS QDs was determined to be 2.1 ± 0.1 nm by transmission electron microscopy (TEM, Fig. S3). PbS QDs show the first exciton absorption band with the tail to 890 nm (bottom of Fig. 2a) and a molar extinction coefficient of 2.74×10^4 L mol^{-1} cm^{-1} at 808 nm, which is over 6-fold higher than that of the Os complex (about 4×10^3 L mol^{-1} cm^{-1}) as the NIR sensitizer.[22] The emission band of PbS QDs peaked at ~825 nm with a PLQY of 68.2%.

The carboxyl functional group enables 3-PYCA to anchor onto the surface of PbS QDs, allowing triplet excitons to be harvested and transferred to form long-lived triplet 3-PYCA *via* Dexter-type TET. Surface loading of 3-PYCA was achieved through a ligand-exchange approach (Section 1.3 in the SI). The average number of 3-PYCAs bound per QD is estimated to be about 10 (Section 1.5 in the SI). The absorption and PL spectra of PbS QDs before and after 3-PYCA functionalization are shown in Fig. 2b. The typical absorption features of both PbS QDs and 3-PYCA are maintained, but a small blue shift (~6 nm) of the absorption bands of 3-PYCA was observed (Fig. S4). This may be because the electronic structure of 3-PYCA is slightly altered by PbS QDs.[34] The PL intensity of PbS QDs reduces significantly when 3-PYCA is attached, with a quenching efficiency of ~90%, which can be attributed to the proposed TET_1 process.

TET from PbS QDs to 3-PYCA

Transient PL and absorption spectroscopies were employed to further investigate the energy transfer from QDs to 3-PYCA. As shown in Fig. 2c, the PL lifetime of PbS QDs attached with 3-PYCA decays much faster than that of PbS QDs alone. The average PL lifetime of only PbS QDs was determined to be 1.85 μs, while that of the ligand-exchanged PbS QDs was only 53 ns (fitting detailed in Section 2.5 of the SI), yielding in a 97% quenching of PL lifetime. Fig. 2d and e shows the femtosecond transient absorption (fsTA) spectra of PbS QDs and PbS QDs anchored with 3-PYCA. Upon the 800 nm pulsed excitation, the PbS QDs exhibit a long-lived exciton bleach (XB) centered at 710 nm and a broad featureless excited-state absorption (ESA) below 650 nm, consistent with previous reports.[35] When anchored with 3-PYCA, both XB and ESA processes are significantly accelerated. Compared with the long-lived XB of PbS QDs for over 500 ns, the time-resolved XB decays of PbS QDs/3-PYCA at 720 nm indicates a significantly shortened lifetime of 322.4 ps (Fig. S5). Notably, at later times (>5.5 ns), a new positive transient band emerges with the maximum between 530 and 550 nm. This new species can be assigned to the triplet excited state of 3-PYCA. Nanosecond transient absorption (nsTA) was

performed to further investigate the energy transfer from PbS QDs to 3-PYCA. As shown in Fig. 2f, the nsTA spectrum of PbS QDs/3-PYCA at 100 ns exhibits a positive transient absorption band with a peak at 530 nm, which also corresponds to the observation in the fsTA. The time-resolved TA at 530 nm (insert in Fig. 2f) shows a long-lived lifetime of 2.29 μs, which can be assigned to the T_1 to T_n absorption of 3-PYCA, similar to the TA signal of previously reported perylene.[36] These results confirm the formation of triplet 3-PYCA *via* TET_1 from PbS QDs, thereby enabling the subsequent endergonic TET_2 step to perylene annihilators.

UC properties of a system consisting of perylene, 3-PYCA and PbS QDs. The TTA-UC performance of our design was investigated by mixing PbS QD anchored 3-PYCA with perylene as the annihilator (sample preparation in Section 1.4 of the SI). Notably, although there is an endergonic energy gap (0.06 eV) between 3-PYCA and perylene, efficient TET can still occur due to the high concentrated perylene in the TTA-UC solution. The UC spectrum in toluene under 808 nm light irradiation is shown in Fig. 3a, and blue emission from the solution was clearly observed (insert in Fig. 3a). Notably, the first UC emission band peaks at 455 nm positioned in the deep-blue region. Comparing the TTA-UC spectrum of perylene (Fig. 3a) with its intrinsic fluorescence spectrum (Fig. S6), the reduced intensity of the first peak is attributed to reabsorption at high concentration. The deep-blue emission from the TTA-UC process can be further enhanced by using a short-path sample holder. When increasing the light intensity of 808 nm excitation, the enhancement of TTA-UC intensity can be observed. Power-dependence of TTA-UC intensity shows a transition from a quadratic to a linear regime as expected (Fig. S7), which is a key characteristic of TTA-UC systems.[37] The excitation threshold of our TTA-UC system was determined to be 5.2 W cm^{-2}. The TTA-UC emission of perylene was also confirmed by determining the PL lifetime. Fig. 3b shows the time-resolved PL decay of perylene at 470 nm in the TTA-UC solution, which is much longer than the lifetime (4.05 ns) of perylene directly upon UV or blue light irradiation. The UC emission of perylene shows an increasing PL lifetime of 3.74 μs and a PL decay lifetime of 30.3 μs, which is because the TET and annihilation processes occur in the microsecond timescale.

The UCQY of NIR-to-deep-blue TTA-UC was determined to be 2.1% in 1,2-dichlorobenzene (out of a 50% maximum, Section 2.3 of the SI), which is about 10-fold higher than those previously reported for QD-based TTA-UC systems that achieved anti-Stokes shifts beyond 0.8 eV.[24,38] Due to the partial spectral overlap between 3-PYCA absorption and perylene emission (Fig. 2a and b), back Förster resonance energy transfer (back-FRET) from perylene to 3-PYCA is expected to reduce PL and thus lower the overall UCQYs. To quantify this loss pathway, we performed control experiments in which the PL spectra and lifetime of 20 mM perylene were measured before and after addition of 100 μM 3-PYCA with the concentration similar to TTA-UC measurement, and the results are shown in Fig. S8 and S9. Upon addition of 3-PYCA, the PL intensity of perylene decreases by approximately 4%. The corresponding PL lifetime of concentrated perylene reduced from 5.84 ns to 5.35 ns, indicating a quenching efficiency of about 8%. Therefore, the back-FRET-induced loss in UCQY contributes to a reduction of less than 8%, as 3-PYCA is confined to the surface of PbS QDs rather than undergoing free diffusion as in these control experiments. Rubrene as the commonly used annihilator for NIR-to-yellow TTA-UC was also employed to pair with our PbS QDs/3-PYCA sensitizers. Under 808 nm light excitation, NIR-to-yellow TTA-UC was observed as expected (Fig. S10) and the UCQY was determined to be 6.35%, which is comparable to the highest record of PbS QD-based TTA-UC to the yellow region.[24]

TTA-UC activated photoisomerization. The large anti-Stokes shift of UC from NIR to deep-blue photons motivated us to exploit its potential for activating photochemical reactions. Azo, a well-known molecular photoswitch, undergoes reversible photoisomerization between *trans* and *cis* isomers (Fig. 4a).[39–43] The *cis*-to-*trans* isomerization of Azo can be induced either by 450 nm blue-light irradiation *via* singlet excited state or slow thermal relaxation *via* the ground state. This photoisomerization process is accompanied by an increase in the absorption band at 280–360 nm (Fig. S11).[44] It is highly desired to activate the photoisomerization of Azo under low-energy photons, especially NIR photons, for deep-penetration applications.[45] To this end, our TTA-UC solution was mixed with Azo (200 μM), and the absorption spectra in the UV region are

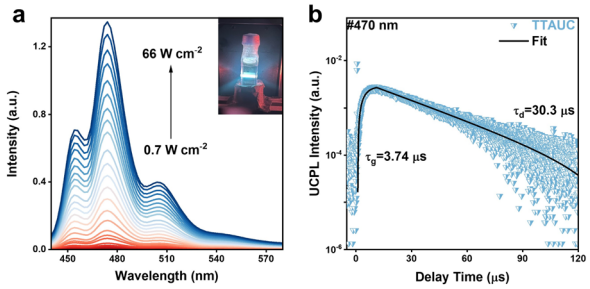

Fig. 3 (a) TTA-UC PL spectra of perylene under 808 nm light irradiation with varied excitation density. The inset photograph shows the deep blue emission generated in the cuvette. (b) Time-resolved PL decay of TTA-UC at 470 nm.

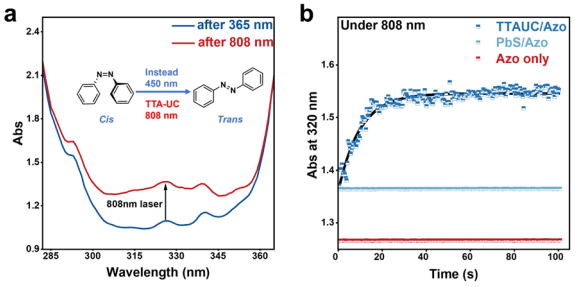

Fig. 4 (a) Absorption spectra of the TTA-UC solution mixed with *cis*-Azo in the UV region and after 808 nm irradiation. (b) The time-dependent *cis*-to-*trans* isomerization followed at absorbance changes at 320 nm under 808 nm irradiation of Azo alone (red), Azo mixed with PbS QDs (light blue) and mixed with TTA-UC solution (deep blue).

shown in Fig. 4a. Upon 808 nm light irradiation (1.2 W, 3 min), an increase in absorbance at 280–360 nm (red spectrum in Fig. 4a) indicates the occurrence of *cis*-to-*trans* isomerization, which is the same as the observation directly under 450 nm light irradiation. It should be noted that no obvious spectral changes were observed for *cis*-Azo alone without TTA-UC solution upon 808 nm irradiation (Fig. S12), which is expected as the photon energy is insufficient to access the singlet excited state of *cis*-Azo; nor did it promote thermal relaxation at room temperature during the irradiation period. The *cis*-to-*trans* photoisomerization kinetics were monitored by tracking absorption changes at 320 nm (Fig. 4b). No obvious changes were observed for Azo alone and Azo mixed with only PbS QDs during 100 s of NIR irradiation. In contrast, when mixed with the TTA-UC solution, it exhibits a rapid increase in absorption within the first 20 s with a growth lifetime of only 9.8 s. Therefore, it demonstrates that deep-blue photons generated from PbS QDs and perylene derivatives *via* TTA-UC can successfully activate the high-energy photoreactions, such as *cis*-to-*trans* isomerization of Azo.

Conclusions

In summary, we have developed a NIR-to-deep-blue TTA-UC system by engineering PbS QDs and perylene derivatives, with an exceptionally large anti-Stokes shift of 1.3 eV. The excellent performance is attributed to the precise alignment of the T_1 energy levels, with only a 0.06 eV offset between PbS QDs, 3-PYCA as the mediator and perylene as the annihilator. Despite the small driving energy force, the efficiency of the TET process is over 90%, as evidenced by steady-state and time-resolved PL, as well as transient absorption spectroscopy. Importantly, the upconverted deep-blue photons generated from our TTA-UC system upon NIR excitation are capable of activating diverse photochemical reactions. As a proof of concept, we demonstrate that *cis*-to-*trans* photoisomerization of Azo can be induced upon 808 nm irradiation, highlighting the potential of TTA-UC for solar energy harvesting in high-energy photon-activated processes.

Author contributions

L. H., H. L. and Q. L. conceived the concept and designed the project. S. Z. carried out PbS QD material synthesis. L. X. and Q. L. performed material characterization tests. H. L. did DFT calculations. H. L. and Q. L. wrote the paper. H. L., Q. L., and Y. F. conducted photoisomerization experiments. All authors discussed the results and commented on the manuscript.

Conflicts of interest

There are no conflicts to declare.

Data availability

The data supporting this article have been included as part of the supplementary information (SI). Supplementary information: sample preparation, instrumentation and optical measurements, theoretical calculation, data characterization, and supporting figures and tables. See DOI: https://doi.org/10.1039/d5sc09759b.

Acknowledgements

The authors acknowledge funding from the National Key Research and Development Project of China (2023YFB3609300); National Natural Science Foundation of China (62205240 and 12274320); Seed Foundation of Tianjin University; Genie Program of Chalmers Foundation in Sweden.

Notes and references

1 C. Simpson, T. M. Clarke, R. W. MacQueen, Y. Y. Cheng, A. J. Trevitt, A. J. Mozer, P. Wagner, T. W. Schmidt and A. Nattestad, An intermediate band dye-sensitised solar cell using triplet–triplet annihilation, *Phys. Chem. Chem. Phys.*, 2015, **17**, 24826–24830.
2 T. F. Schulze, J. Czolk, Y.-Y. Cheng, B. Fückel, R. W. MacQueen, T. Khoury, M. J. Crossley, B. Stannowski, K. Lips, U. Lemmer, A. Colsmann and T. W. Schmidt, Efficiency Enhancement of Organic and Thin-Film Silicon Solar Cells with Photochemical Upconversion, *J. Phys. Chem. C*, 2012, **116**, 22794–22801.
3 T. Morifuji, Y. Takekuma and M. Nagata, Integrated Photon Upconversion Dye-Sensitized Solar Cell by Co-adsorption with Derivative of Pt–Porphyrin and Anthracene on Mesoporous TiO2, *ACS Omega*, 2019, **4**, 11271–11275.
4 Z. Huang, C.-H. Tung and L.-Z. Wu, Quantum Dot-Sensitized Triplet–Triplet Annihilation Photon Upconversion for Solar Energy Conversion and beyond, *Acc. Mater. Res.*, 2024, **5**, 136–145.
5 O. S. Kwon, H. S. Song, J. Conde, H.-I. Kim, N. Artzi and J.-H. Kim, Dual-Color Emissive Upconversion Nanocapsules for Differential Cancer Bioimaging In Vivo, *ACS Nano*, 2016, **10**, 1512–1521.
6 L. Huang, L. Zeng, Y. Chen, N. Yu, L. Wang, K. Huang, Y. Zhao and G. Han, Long wavelength single photon like driven photolysis via triplet triplet annihilation, *Nat. Commun.*, 2021, **12**, 122.
7 V. Gray, K. Moth-Poulsen, B. Albinsson and M. Abrahamsson, Towards efficient solid-state triplet–triplet annihilation based photon upconversion: Supramolecular, macromolecular and self-assembled systems, *Coord. Chem. Rev.*, 2018, **362**, 54–71.
8 S. N. Sanders, T. H. Schloemer, M. K. Gangishetty, D. Anderson, M. Seitz, A. O. Gallegos, R. C. Stokes and D. N. Congreve, Triplet fusion upconversion nanocapsules for volumetric 3D printing, *Nature*, 2022, **604**, 474–478.
9 D. K. Limberg, J.-H. Kang and R. C. Hayward, Triplet–Triplet Annihilation Photopolymerization for High-Resolution 3D Printing, *J. Am. Chem. Soc.*, 2022, **144**, 5226–5232.
10 J. Zhou, Q. Liu, W. Feng, Y. Sun and F. Li, Upconversion Luminescent Materials: Advances and Applications, *Chem. Rev.*, 2014, **115**, 395–465.

11 N. Weitzel, A. Tsutskiridze, J. Bramowski, B. König and T. Hirsch, Fully Sensitized Upconversion Nanoparticles as Efficient Catalysts for NIR-Driven UV Photochemistry, *Angew. Chem., Int. Ed.*, 2025, **64**, e202511247.
12 S. Geng, H. Li, Z. Lv, Y. Zhai, B. Tian, Y. Luo, Y. Zhou and S. T. Han, Challenges and Opportunities of Upconversion Nanoparticles for Emerging NIR Optoelectronic Devices, *Adv. Mater.*, 2025, **37**, 2419678.
13 P. Bharmoria, H. Bildirir and K. Moth-Poulsen, Triplet–triplet annihilation based near infrared to visible molecular photon upconversion, *Chem. Soc. Rev.*, 2020, **49**, 6529–6554.
14 K. Chen, Q. Luan, T. Liu, B. Albinsson and L. Hou, Semiconductor nanocrystals-based triplet-triplet annihilation photon-upconversion: Mechanism, materials and applications, *Responsive Mater.*, 2024, **3**, e20240030.
15 C. Mongin, S. Garakyaraghi, N. Razgoniaeva, M. Zamkov and F. N. Castellano, Direct observation of triplet energy transfer from semiconductor nanocrystals, *Science*, 2016, **351**, 369–372.
16 M. W. Brett, C. K. Gordon, J. Hardy and N. J. L. K. Davis, The Rise and Future of Discrete Organic–Inorganic Hybrid Nanomaterials, *ACS Phys. Chem. Au*, 2022, **2**, 364–387.
17 J. T. DuBose and P. V. Kamat, Efficacy of Perovskite Photocatalysis: Challenges to Overcome, *ACS Energy Lett.*, 2022, **7**, 1994–2011.
18 R. Weiss, Z. A. VanOrman, C. M. Sullivan and L. Nienhaus, A Sensitizer of Purpose: Generating Triplet Excitons with Semiconductor Nanocrystals, *ACS Mater. Au*, 2022, **2**, 641–654.
19 N. A. Romero and D. A. Nicewicz, Organic Photoredox Catalysis, *Chem. Rev.*, 2016, **116**, 10075–10166.
20 Z. Wang, M. Wu, X. Cui, F. Ge, P. Xiao, M. Li and H. Fu, Triplet–Triplet Annihilation Upconversion with Large Anti-Stokes Shift, *ACS Nano*, 2025, **19**, 25596–25616.
21 T. N. Singh-Rachford, A. Nayak, M. L. Muro-Small, S. Goeb, M. J. Therien and F. N. Castellano, Supermolecular-Chromophore-Sensitized Near-Infrared-to-Visible Photon Upconversion, *J. Am. Chem. Soc.*, 2010, **132**, 14203–14211.
22 S. Amemori, Y. Sasaki, N. Yanai and N. Kimizuka, Near-Infrared-to-Visible Photon Upconversion Sensitized by a Metal Complex with Spin-Forbidden yet Strong S0-T1 Absorption, *J. Am. Chem. Soc.*, 2016, **138**, 8702–8705.
23 X. Wang, F. Ding, T. Jia, F. Li, X. Ding, R. Deng, K. Lin, Y. Yang, W. Wu, D. Xia and G. Chen, Molecular near-infrared triplet-triplet annihilation upconversion with eigen oxygen immunity, *Nat. Commun.*, 2024, **15**, 2157.
24 L.-H. Jiang, X. Miao, M.-Y. Zhang, J.-Y. Li, L. Zeng, W. Hu, L. Huang and D.-W. Pang, Near Infrared-II Excited Triplet Fusion Upconversion with Anti-Stokes Shift Approaching the Theoretical Limit, *J. Am. Chem. Soc.*, 2024, **146**, 10785–10797.
25 Z. Ju and R. Deng, Cascade Lanthanide-Triplet Energy Transfer for Nanocrystal-Sensitized Organic Photon Upconversion, *Angew. Chem., Int. Ed.*, 2025, **64**, e202422575.
26 H. Wang, J. Ponmani, N. Sangaraiah, J. Meng and C. Zhou, Current Researches and Applications of Perylene Compounds, *Prog. Chem.*, 2015, **27**, 704–743.
27 C. Li and H. Wonneberger, Perylene Imides for Organic Photovoltaics: Yesterday, Today, and Tomorrow, *Adv. Mater.*, 2012, **24**, 613–636.
28 L. Naimovičius, E. Radiunas, M. Dapkevičius, P. Bharmoria, K. Moth-Poulsen and K. Kazlauskas, The statistical probability factor in triplet mediated photon upconversion: a case study with perylene, *J. Mater. Chem. C*, 2023, **11**, 14826–14832.
29 A. Hamasaki, K. Kubo, M. Harashima, A. Katsuki and S. Ozeki, Reversible Change between Excimer and Monomer Forms of Perylene Induced by Water Absorption and Dehydration of Poly-N-isopropylacrylamide Gel, *J. Phys. Chem. B*, 2021, **125**, 2987–2993.
30 Q. Zhou, M. Zhou, Y. Wei, X. Zhou, S. Liu, S. Zhang and B. Zhang, Solvent effects on the triplet-triplet annihilation upconversion of diiodo-Bodipy and perylene, *Phys. Chem. Chem. Phys.*, 2017, **19**, 1516–1525.
31 X. Cui, A. Charaf-Eddin, J. Wang, B. Le Guennic, J. Zhao and D. Jacquemin, Perylene-Derived Triplet Acceptors with Optimized Excited State Energy Levels for Triplet–Triplet Annihilation Assisted Upconversion, *J. Org. Chem.*, 2014, **79**, 2038–2048.
32 T. N. Singh-Rachford and F. N. Castellano, Triplet Sensitized Red-to-Blue Photon Upconversion, *J. Phys. Chem. Lett.*, 2009, **1**, 195–200.
33 W. Huang, S. Wang, H. Gong, J. Tian, J. Peng and J. Cao, Size tunable and controllable synthesis of PbS quantum dots for broadband photoelectric response, *Opt. Mater.*, 2023, **142**, 113977.
34 R. Sun, J. Zang, R. Lai, W. Yang and B. Ji, Near-Infrared-to-Visible Photon Upconversion with Efficiency Exceeding 21% Sensitized by InAs Quantum Dots, *J. Am. Chem. Soc.*, 2024, **146**, 17618–17623.
35 Z. Huang, Z. Xu, M. Mahboub, Z. Liang, P. Jaimes, P. Xia, K. R. Graham, M. L. Tang and T. Lian, Enhanced Near-Infrared-to-Visible Upconversion by Synthetic Control of PbS Nanocrystal Triplet Photosensitizers, *J. Am. Chem. Soc.*, 2019, **141**, 9769–9772.
36 K. Kumar Jha, A. Prabhakaran, R. Cane Sia, R. A. Arellano Reyes, N. Kumar Sarangi, T. Yang, K. Kumar, S. Kupfer, J. Guthmuller, T. E. Keyes and B. Dietzek-Ivanšić, Triplet Formation and Triplet-Triplet Annihilation Upconversion in Iodine Substituted Non-Orthogonal BODIPY-Perylene Dyads, *ChemPhotoChem*, 2023, **7**, e202300073.
37 F. Edhborg, A. Olesund and B. Albinsson, Best practice in determining key photophysical parameters in triplet-triplet annihilation photon upconversion, *Photochem. Photobiol. Sci.*, 2022, **21**, 1143–1158.
38 N. Nishimura, J. R. Allardice, J. Xiao, Q. Gu, V. Gray and A. Rao, Photon upconversion utilizing energy beyond the band gap of crystalline silicon with a hybrid TES-ADT/PbS quantum dots system, *Chem. Sci.*, 2019, **10**, 4750–4760.
39 Z. Ziani, C. Bellatreccia, F. P. Battaglia, G. Morselli, A. Gradone, P. Ceroni and M. Villa, Copper indium sulfide

quantum dots enabling quantitative visible light photoisomerisation of (E)-azobenzene chromophores, *Nanoscale*, 2024, **16**, 12947–12956.

40 M.-A. Morikawa, M. Mizuno, N. Harada and N. Kimizuka, On-demand Triplet-sensitized Photoswitching of Arylazopyrazoles, *Chem. Lett.*, 2023, **52**, 727–731.

41 J. Isokuortti, K. Kuntze, M. Virkki, Z. Ahmed, E. Vuorimaa-Laukkanen, M. A. Filatov, A. Turshatov, T. Laaksonen, A. Priimagi and N. A. Durandin, Expanding excitation wavelengths for azobenzene photoswitching into the near-infrared range via endothermic triplet energy transfer, *Chem. Sci.*, 2021, **12**, 7504–7509.

42 P. Bharmoria, S. Ghasemi, F. Edhborg, R. Losantos, Z. Wang, A. Mårtensson, M.-A. Morikawa, N. Kimizuka, Ü. İşci, F. Dumoulin, B. Albinsson and K. Moth-Poulsen, Far-red triplet sensitizedZ-to-Ephotoswitching of azobenzene in bioplastics, *Chem. Sci.*, 2022, **13**, 11904–11911.

43 Y. Feng, Q. Luan, S. Zhang, L. Xi, S. Zhang, K. Chen, T. Liu and L. Hou, Near-infrared light-activated Z-to-E isomerization of azobenzene via triplet sensitization from PbS quantum dots, *Chem. Sci.*, 2025, **16**, 16151–16157.

44 L. Naimovičius, M. Miroshnichenko, E. Opar, H. Hölzel, M.-A. Morikawa, N. Kimizuka, M. Dapkevičius, J. Lekavičius, E. Radiunas, K. Kazlauskas, V. Cilleros-Mañé, F. Riefolo, C. Matera, K. Harmandar, M. Taniguchi, F. Dumoulin, J. S. Lindsey, P. Bharmoria, P. Gorostiza and K. Moth-Poulsen, Noninvasive cardiac modulation via triplet-sensitized photoswitching in the phototherapeutic window, *Nat. Commun.*, 2025, **16**, 6377.

45 H. B. Cheng, S. Zhang, J. Qi, X. J. Liang and J. Yoon, Advances in Application of Azobenzene as a Trigger in Biomedicine: Molecular Design and Spontaneous Assembly, *Adv. Mater.*, 2021, **33**, e2007290.